A simple route to controllable growth of ZnO nanorod arrays on conducting substrates

Y. Jiao[abc], **H. J. Zhu**[a], **X. F. Wang**[b], **L. Shi**[d], **Y. Liu**[e], **L. M. Peng**[e]**andQuan Li***[ab]

[a]*Department of Physics, The Chinese University of Hong Kong, Shatin, New Territory, Hong Kong, China. E-mail: liquan@phy.cuhk.edu.hk*

[b]*Shenzhen Institute of Advanced Technology, Chinese Academy of Science, ShenZhen, China*

[c]*Department of Physics, North West University, Xi'an, 710069, China*

[d]*Department of Chemistry, University of Science and Technology of China, Hefei, 230026, China*

[e]*Department of Electronics, Peking University, Beijing, China*

Received 4th September 2009, Accepted 23rd October 2009First published on the web 18th November 2009

Aligned ZnO nanorod arrays are grown on Zn foil using a simple and low cost solution chemistry approach. We have studied the effects of various growth parameters, including the temperature, solution composition and the concentration of individual components on the morphology, structural quality, and properties of the ZnO nanorods. The average diameter of the nanorods in the array can be tuned from ~20 nm to ~150 nm by systematically changing the growth conditions. We found that nanorods with larger diameters are of better structural quality as compared to the smaller diameter ones, as suggested by the cathodoluminescence measurement of these nanorods. Electrical measurements performed on individual ZnO nanorod-on-Zn substrate reveal ohmic contact between them. By pre-depositing a Zn layer (with controlled thickness) on other conducting substrates, such as Cu, ZnO nanorod arrays can be grown on a number of

different substrates using a similar method.

1. Introduction

Zinc oxide has received wide attention as a promising functional semiconductor material for many years. It possesses a wide band gap (3.37 eV at room temperature) and large exciton binding energy (60 meV), making it a competitive candidate for applications in blue-UV light emission and room temperature UV lasing.[1] It is a well-known piezoelectric material in surface acoustic wave devices for delay lines, filters, resonators in wireless communication, and signal processing.[2,3] It also enjoys a fairly simple crystal-growth technology, which results in a potentially lower cost for ZnO-based devices.[4] Moreover, it is environmentally stable as well as biocompatible.[5]

Recently, one-dimensional (1D) ZnO nanostructures attract considerable research interest due to the inspiring idea of building electronic devices at the nanometre scale using the bottom-up approach. Much effort has been devoted to the fabrication of quasi-one-dimensional ZnO nanostructures with different morphologies such as nanobelts, nanorods, and nanotubes. Several devices employing ZnO 1D nanostructures as the major functional units have been demonstrated, including solar cell, sensor, and piezoelectric nanogenerator.[6–9] In particular, aligned ZnO nanorod arrays on conducting substrates are of special interests, as it can serve as nanoelectrode for many optoelectronic applications.[10]

In the present work, we have employed a simple and low cost method to grow aligned ZnO nanorod arrays on Zn foil. The average diameter of the nanorods can be tuned from 20 nm to 150 nm by varying the growth conditions. Both optical and electrical properties of these nanorods have been studied and discussed by correlating them to the structural quality of the nanorods. In addition, we have applied such a growth methodology to different conducting substrate by depositing a Zn layer on them. The Cu foil has been used as an example in illustrating such a method.

2. Experiment

A general procedure to synthesize ZnO nanorod arrays can be found in the following: a mixture of 10 mL NaOH and 5 mL H_2O_2 aqueous solution is firstly added in a 20 mL stainless steel Teflon-lined autoclave. A piece of 2 cm × 2.5 cm zinc foil is then added to the above solution before the autoclave is sealed. The autoclave is then kept at a constant temperature for several hours before returning the system to room temperature. Finally, the zinc foil is taken out of the solution, rinsed with distilled water and dried in air. We have identified three synthesis parameters that would affect the morphology and structural quality of the ZnO nanorod arrays, *i.e.* the concentration of H_2O_2 and NaOH in the solution, the concentration ratio of H_2O_2 to NaOH, as well as the growth temperature.

The plating of zinc film on the Cu substrate is carried using an acidic zinc chloride solution. The electrolyte contains 60 g L^{-1} $ZnCl_2$ (Merck, reagent grade) and 200 g L^{-1} KCl (Merck, reagent grade) which are dissolved in the de-ionized water. 20–30 g L^{-1} H_3BO_3 is then added to the electrolyte to adjust the pH value at 4.8–5.1. Zn sheet is used as the anode and Cu sheet, about the

same size and shape as the Zn sheet, is used as cathode. Both sheets are cleaned in acetone and alcohol in a sequential manner, and an additional treatment of the Cu substrate in the 10% HCl has been performed before the plating. During the plating, a constant current with a current density of 5–10 A dm^{-2} is maintained for 30 s to 2 min. The surface of as-deposit Zn layer on Cu is mechanically polished to be flattened. Finally, the substrate is cleaned in the DI water and dried by heating to ~150 °C for 15 min. The thickness of the Zn film is estimated based on the profilometry measurement after the Zn film is polished.

The general morphology and crystallinity of the products were examined using scanning electron microscopy (FESEM QF400) and X-ray diffraction (XRD). Transmission electron microscopy (TEM Tecnai 20ST) related techniques were employed to investigate the detailed microstructure of the products. The luminescence properties of the as-synthesized nanorod arrays were examined at room temperature using a Mono CL system attached to a SEM (MonoCL Oxford Instrument). A four nanoprobes (MM3A, Kleindiek Company) SEM system (FEI XL 30F) was used to perform transport measurements on both the single ZnO nanorod and the single junction in between the nanorod and the Zn substrate, and a W tip was used.

3. Results

Fig. 1 shows the SEM images of the samples synthesized with different solution composition but at the same temperature (150 °C) and for the same duration (2 h). Three different solution compositions have been used: (a) 5 mL 1% H_2O_2 and 10 mL 2M NaOH, (b) 5 mL 0.5% H_2O_2 and 10 mL 2M NaOH and (c) 5 mL 0.25% H_2O_2 and 10 mL 2M NaOH. Thick nanorods are obtained for both (a) and (b) with a large non-uniformity existing in the nanorod diameters. These nanorods are composed of O and Zn, as suggested by the EDX analysis (Fig. 2a). XRD spectra taken from these specimens reveal the wurtzite structure of the nanorods (Fig. 2b). A slight decrease in the average diameter of these nanorods is observed when the H_2O_2 concentration is reduced from 1% to 0.5%. Nevertheless, when the H_2O_2 concentration is further reduced to 0.25% and below, no obvious nanorod growth is observed on the Zn foil. Instead, a rough surface (Fig. 1c) composed of Zn and a small amount of O is found.

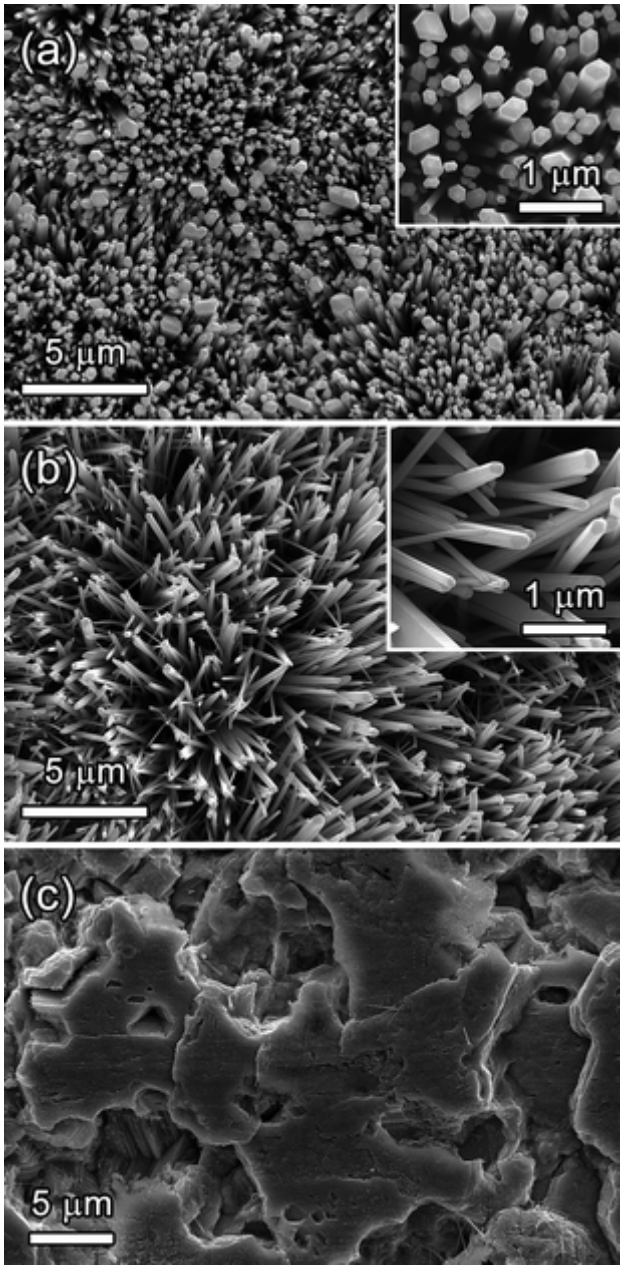

Fig. 1SEM images of samples synthesized in a mixed aqueous solution of (a) 5 mL 1% H_2O_2 and 10 mL 2M NaOH, (b) 5 mL 0.5% H_2O_2 and 10 mL 2M NaOH, and (c) 5 mL 0.25% H_2O_2 and 10 mL 2M NaOH. All solutions were kept at 150 °C for 2 h.

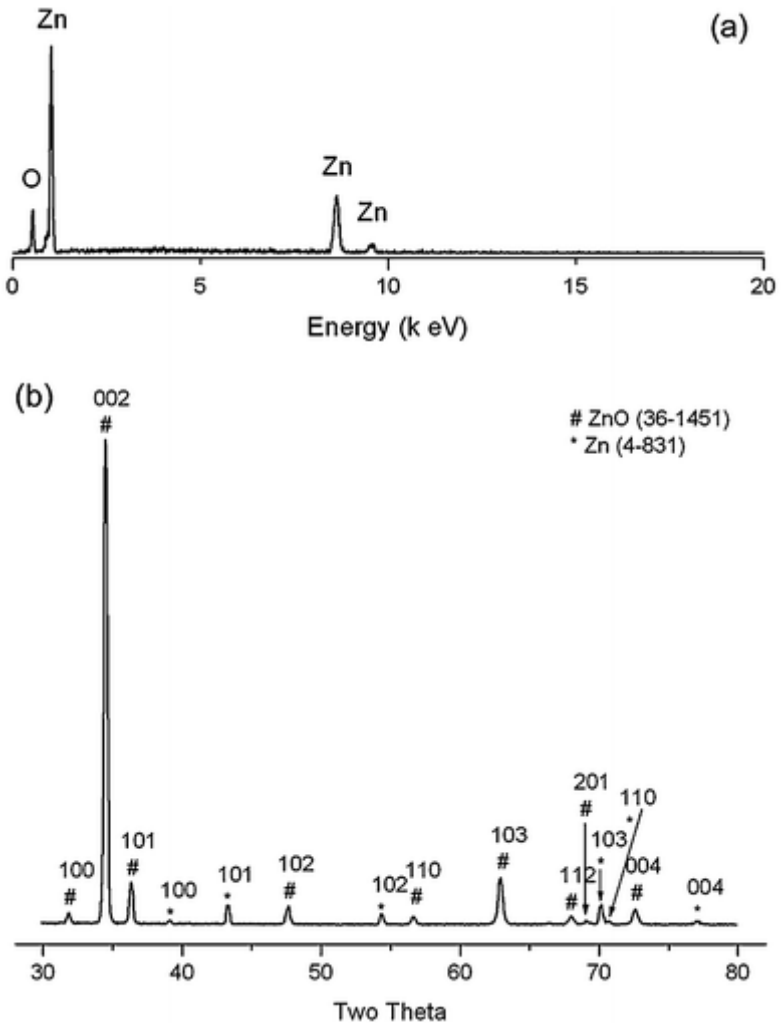

Fig. 2(a) EDX spectrum taken from thick ZnO nanorods on Zn foil; (b) XRD spectrum taken from thick ZnO nanorods on Zn foil.

On the other hand, the morphology of the product is also affected by the concentration ratio of H_2O_2 and NaOH. As we reduce the concentration of NaOH solution to 0.2 M, but keeping H_2O_2 concentration at 0.25%, nanorods start to grow on the Zn foil surface again (Fig. 3). At the same time, uniformity of the nanorod arrays has been improved, with an average diameter being reduced to ~70 nm.

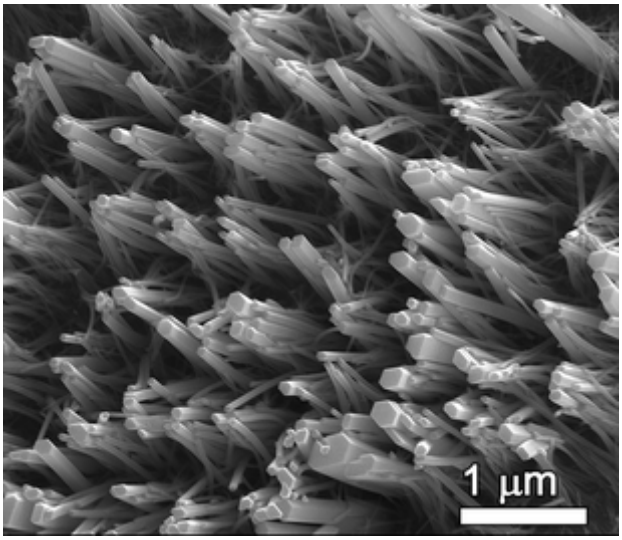

Fig. 3SEM image of specimen synthesized at 150 °C for 2 h, with the mixed aqueous solution of 5 mL 0.25% H_2O_2 and 10 mL 0.2M NaOH.

Temperature is another important factor in tuning the nanorod diameter. In the temperature series, we have fixed the reaction temperature at ~150 °C, ~70 °C, ~21 °C, and ~5 °C, respectively. (The solution consists of 5 mL 0.25% H_2O_2 and 10 mL 0.2M NaOH). We found that the diameter of the ZnO nanorods decreases dramatically with the decreasing of synthesis temperature. At 70 °C, the average diameter of the nanorods is 30 nm (Fig. 4b). When the synthesis temperature goes down to 21 °C, average diameter of the ZnO nanorods is further reduced to around 20 nm. Nevertheless, further reducing the temperature to 5 °C fails to result in ZnO nanorod of any smaller average diameter. Fig. 5 shows the TEM images taken at the nanorods with small diameters. Each nanorod is single crystalline, with wurtzite ZnO [001] as the growth direction. However, the narrower nanorods are more subjective to electron beam irradiation damage in the TEM. More and more small regions with brighter contrast appear (indicated by arrows in the high resolution image) with the increasing of electron beam illumination time. It is caused by the electron beam sputtering and thinning effect on the specimen.[11]

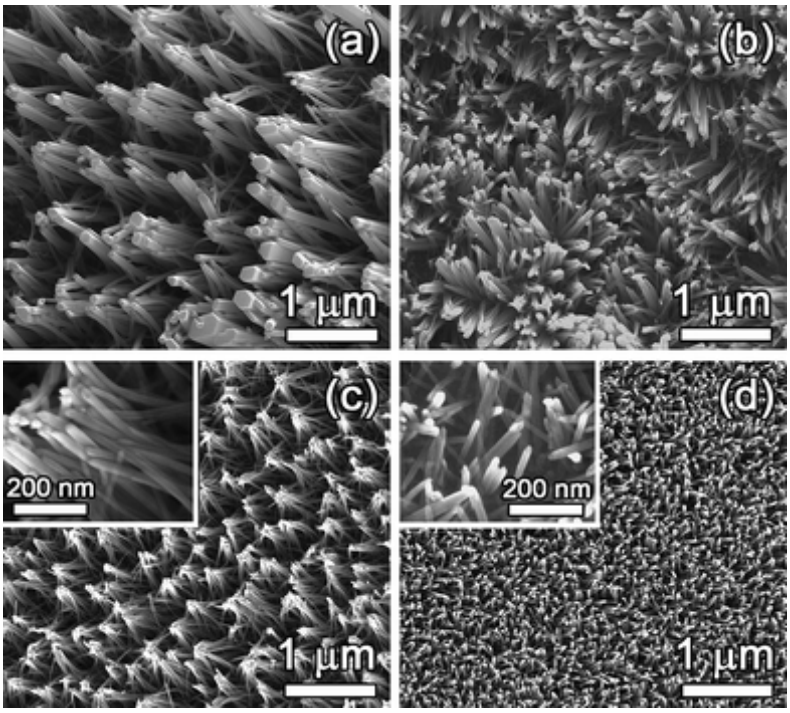

Fig. 4SEM images of samples synthesized at (a) 150 °C (b) 70 °C (c) 21 °C and (d) 5 °C with aqueous solution of 5 mL 0.25% H_2O_2 and 10 mL 0.2M NaOH. Insets are larger magnification images of the corresponding sample.

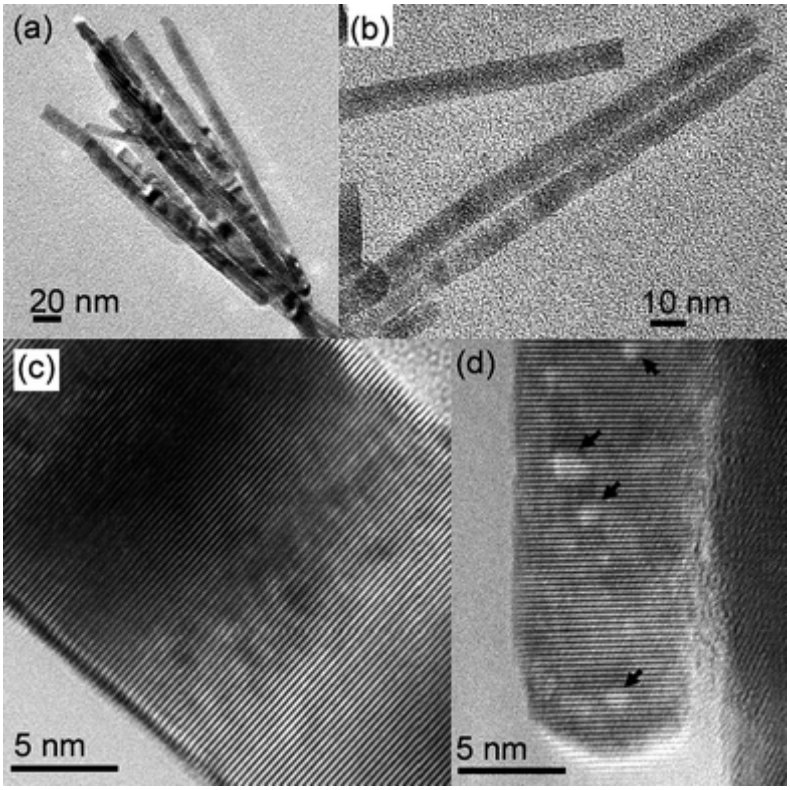

Fig. 5(a), (b) Low magnification TEM images

taken from ZnO nanorods with diameter of 16 nm and 10 nm. (c), (d) high resolution TEM images taken from ZnO nanorods with diameter of 16 nm and 8 nm. Arrows in (d) point to damaged regions on the specimen, which are induced by electron beam irradiation during the observation.

Fig. 6a and 6b show typical cathodoluminescence (CL) spectra taken from ZnO nanorods with average diameter of 120 nm and 30 nm, respectively. Strong band edge emission is always observed when the diameter of the ZnO nanorod is large ($\geq$70 nm). While for nanorods with smaller diameters, band edge emission becomes weak and defect emission dominates in the spectra. The defect emission from the thin nanorods covers a wide wavelength range starting from 450 nm to 800 nm, with maximum at ~600 nm. A similar broad defect emission but with very low intensity centered at ~560 nm can also be observed from the wide nanorods. The yellow and orange emissions are normally assigned to O interstitial or the presence of –OH group; while the green emission may result from Zn vacancy, and O vacancy *etc.*, the origin of which remains controversial.[12,13] The broad non-UV luminescence peak from the specimen indicates that more than one type of defects are involved.

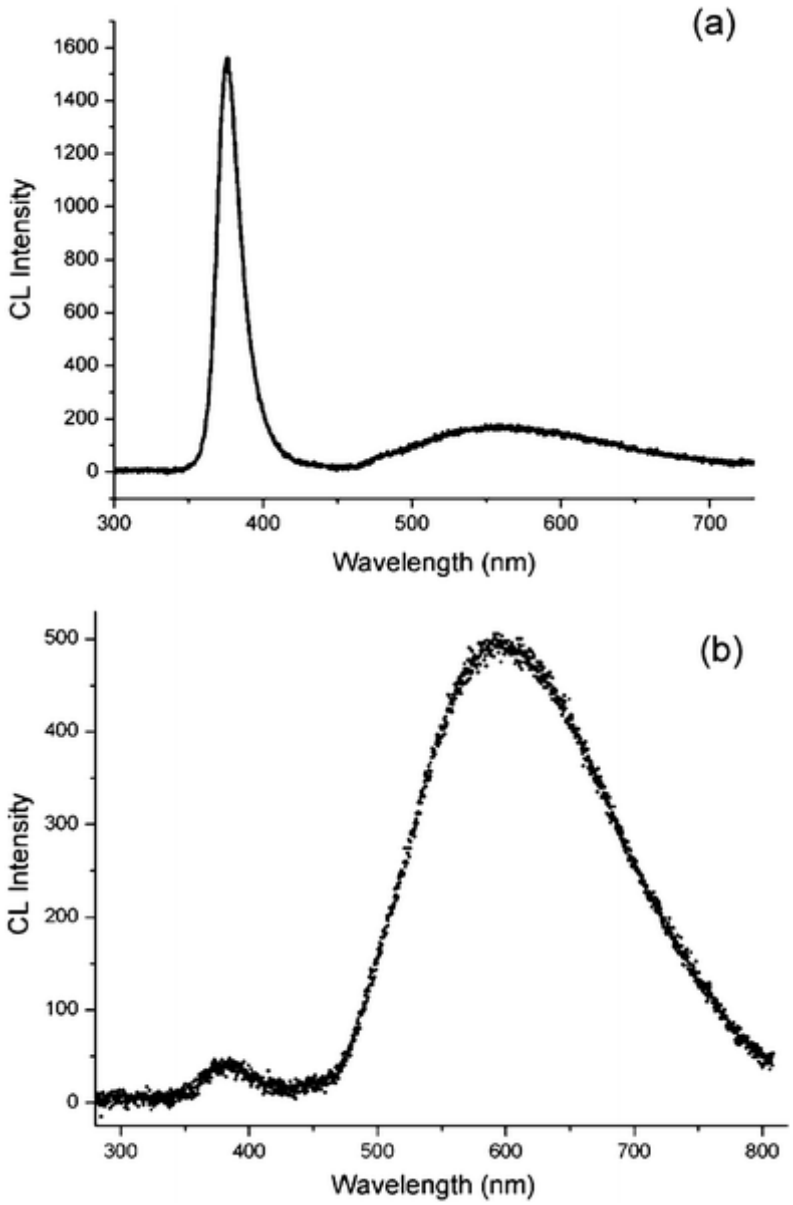

Fig. 6 Room temperature cathodoluminescence spectra taken from the ZnO nanorods with average diameter of (a) ~120 nm and (b) ~30 nm.

The electrical measurements were performed on specimen fabricated at higher temperature (150 °C). The diameter range of the nanorods measured is ~50–250 nm, and similar resistivity has been found in all the nanorods measured. A linear *I–V* characteristic (Fig. 7a) is observed when we locate two probes on the two side of a single nanorod (without touching the Zn substrate). The data is reproducible for all of the ZnO nanorods (several tens of them) measured. Based on the *I–V* data, the resistivity of the nanorods is estimated to be in the order of 10^{-1} Ω cm, which is consistent with that of intrinsic ZnO without intentional doping. The electrical behaviour of the single junction between the ZnO nanorod and the Zn substrate was also measured by fixing one of the probes on the nanorod and another on the conducting substrate. Linear *I–V* characteristic is always found (Fig. 7b). Based on tens of individual nanorods measured, ohmic contact exists

between the ZnO nanorod and Zn substrate.

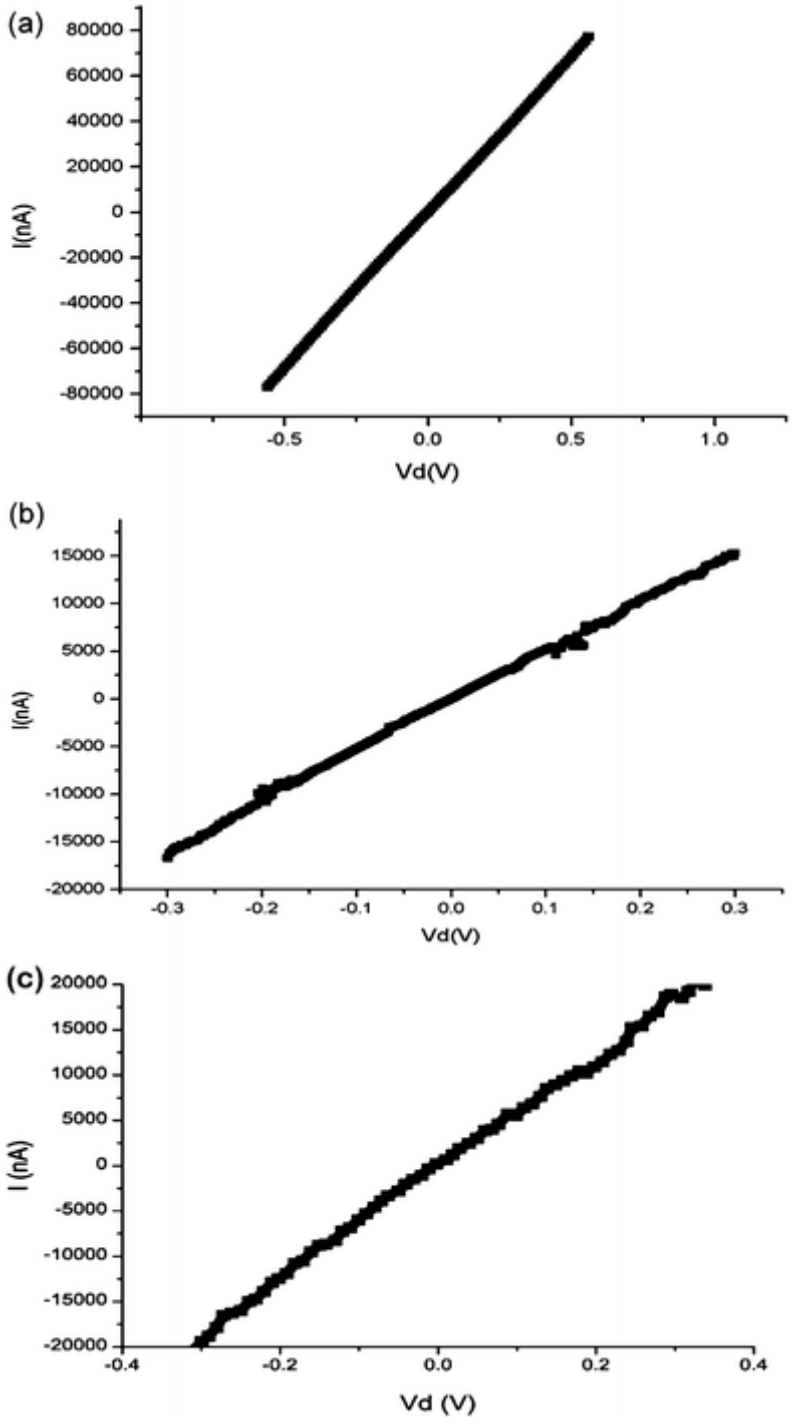

Fig. 7 *I–V* characteristic measured from (a) single ZnO nanorod by locating two probes on the two side of the nanorod (without touching the Zn substrate); (b) the junction between a ZnO nanorod and Zn substrate; and (c) the junction between a ZnO nanorod and Cu substrate by fixing one of the probes on the nanorod and another one on the conducting

substrate.

Such an approach to grow ZnO nanorod arrays can be applied to many other conducting substrates, by pre-depositing a Zn layer with controlled thickness prior to the nanorod growth. The controlled thickness of Zn layer ensures that all the Zn on the substrate can be exhausted for the nanorod growth. Taking Cu substrate as an example, Fig. 8 shows the SEM image of ZnO nanorod arrays grown on the Cu foil. Structure characterizations of these samples show similar behaviour to those grown directly on Zn foil. The transport behaviour of the ZnO nanorods on Cu substrate is very similar to those on the Zn substrate (Fig. 7c), *i.e.*, ohmic contact exist between the nanorod and Cu. As the melting temperature of Cu is much higher than that of Zn, nanorods grown on Cu substrate is expected to be more convenient for further material processing and device applications.

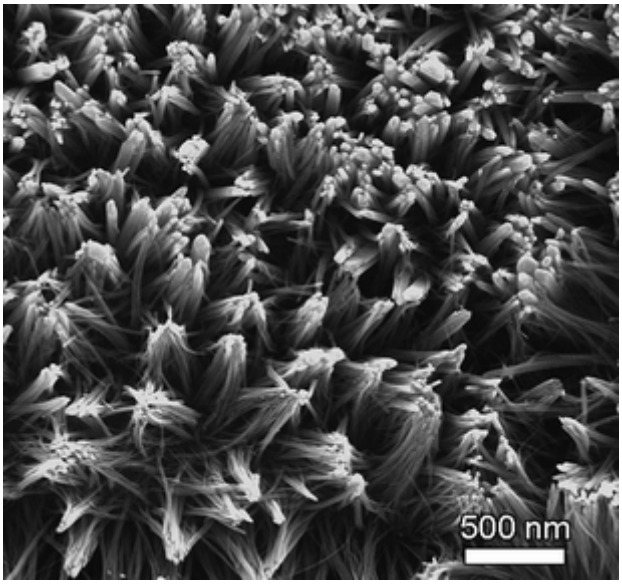

Fig. 8SEM image of ZnO nanorod array growing on Cu foil, which was prepared at 70 °C, with the solution of 5 mL 0.2% H_2O_2 and 10 mL 0.2M NaOH.

4. Discussion

4.1. General growth mechanism of the ZnO nanorod arrays

The growth mechanism of the ZnO array on Zn foil or Cu foil coated Zn is proposed as follows. During our reaction process H_2O_2 decomposes and produces high concentration of oxygen in the sealed system.[14] In the alkaline solution of NaOH with a large amount of oxygen, the Zn foil surface is readily oxidized. This is revealed by the SEM image (Fig. 9a) taken at initial stage of the nanorod growth. Occasionally, through a sparsely packed nanorod array, small particles with diameter around 5 nm can still be observed on the substrate (Fig. 9b). These nanoclusters become the nuclei for further ZnO crystal growth as the oxidation proceeds. It is well known that the ZnO has a natural tendency of anisotropic growth along *c* axis ([001] crystalline direction). In addition,

the produced strong oxidizing environment serves as a kinetic driving force and promotes the anisotropic development and thus the growth of elongated nanocrystals. As a result, ZnO nanorod arrays on Zn foil or Cu foil coated Zn are formed with all of the nanorods growing along the [001] crystalline direction.

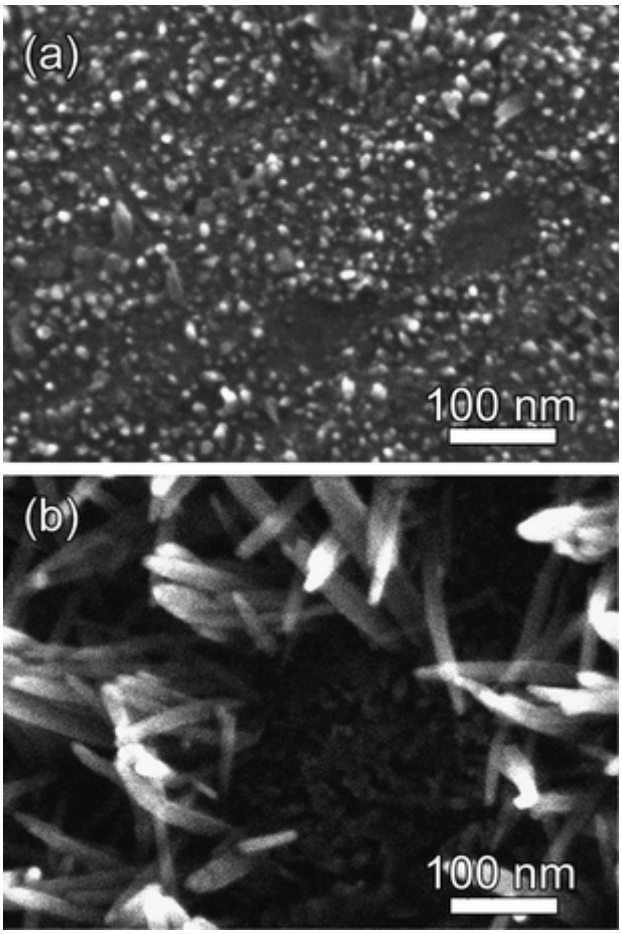

Fig. 9(a) SEM image taken at the initial growth stage of the specimen prepared at 21 °C with aqueous solution of 5 mL 0.5% H_2O_2 and 10 mL 0.2M NaOH. Nanoclusters with diameter around 5 nm cover on the Zn foil surface. (b) Occasionally, through a sparsely packed nanorod array, some nanoclusters on the substrate can still be observed by SEM. The nanorod was prepared at 40 °C with aqueous solution of 5 mL 0.25% H_2O_2 and 10 mL 0.2M NaOH.

4.2. Appropriate concentration ratio between H_2O_2 and NaOH for the nanorod growth

Concentration (or mass) ratio between H_2O_2 and NaOH determines the composition and morphology of the final product. If the ratio is too high (for example, $\geq$5%/0.2 M), the Zn foil is

passivated, with a completely oxidized surface formed soon after the reaction starts. When such a compact ZnO layer immediately forms on surface of the Zn foil, it slows down the further oxidation process of the Zn. More importantly, the ZnO nucleus would fail to form, and thus no further 1D growth. If the H_2O_2/NaOH ratio is too low (for example, 0.25%/2 M), all of the ZnO forming due to oxidation would dissolve in the strong alkaline solution faster than the further formation of ZnO ($ZnO + H_2O + 2OH^- \longrightarrow Zn(OH)_4^{2-}$),[15] leaving an etched Zn surface.

ZnO nanorod arrays only appear at a medium concentration (or mass) ratio between H_2O_2 and NaOH. Under such condition, the ZnO seed layer initially forms on Zn foil surface is not compact, allowing further oxidation of Zn to occur and contribute to the ZnO nanorod growth. The appropriate concentration ratio between H_2O_2 and NaOH for ZnO nanorod arrays growth approximately ranges in 2.5~0.25 (%/M).

4.3. Averaged diameter of the ZnO nanorods

Diameter value of the ZnO nanorods varies with two factors, *i.e.* the concentration of the H_2O_2 solution and the synthesis temperature. High H_2O_2 concentration (for example 1%) produces a great amount of source material in the solution, which allows the nuclei continuously increase their volumes and form nanorods with large average diameter (~150 nm). As the concentration of the H_2O_2 solution decreases, supply of the source material that contributes to ZnO nanorod growth is reduced. It will restrict the augment of the nanorods in both their diameter and length.

Growth rate of the nanorods highly depends on the synthesis temperature. Lowering the temperature effectively slows down the crystal growth process, which makes the products keep at smaller size in both their lateral and longitudinal aspects, as the synthesis process is terminated after a certain period of time.

4.4. Uniformity changing of the ZnO nanorod arrays

Uniformity of the ZnO nanorod arrays is simultaneously affected by the concentration ratio of H_2O_2 to NaOH, the synthesis temperature, as well as surface roughness of the substrate. A higher concentration ratio of H_2O_2 to NaOH (for example, $\geq$1.25%/M) helps to form nanorod arrays with better uniformity. This is because adequate source material is supplied during the nucleation and growth processes of the nanocrystals, which makes the existing seeds on the Zn foil surface grow at similar rate. While the H_2O_2 to NaOH concentration ratio decreases, supply of the source material is limited. It creates local difference on the amount of the source material, which could be increased due to the surface roughness of the Zn foil and/or accelerated dissolving rates at grain boundaries on the foil surface. As a result, the existing seeds on the foil surface grow at different rates, forming nanorods with various diameters. Moreover, as time increases, small sized nanorods may start to dissolve in the solution again and re-grow onto those undissolved larger ones—a mechanism similar to Ostwald ripening.[16] This makes the sizes of tiny crystals reduce while the larger ones increase, further deteriorating the non-uniformity of the nanorod arrays.

For a specified H_2O_2/NaOH ratio, there is a temperature range that makes the nanorod arrays have better uniformity, *e.g.* for 1.25%/M, the temperature range $\leq$70 °C is appropriate. Once the temperature gets too high, the ZnO solubility in the solution is dramatically increased,[17] which equals to a large reduction on the supply of the source material.

At lower temperature ($\leq$70 °C), surface roughness of the Zn foil also becomes a dominant factor that determines the uniformity of the nanorod arrays. With the decreasing of temperature, reactions and diffusion in the solution gradually slow down. The local concentration difference of

the source material is more easily to be produced on a rough substrate surface, worsening the uniformity of the nanorod arrays. Indeed, flattening the Zn foil surface by electro polish or mechanical polish is proved to improve uniformity of the nanorod arrays (Fig. 10).

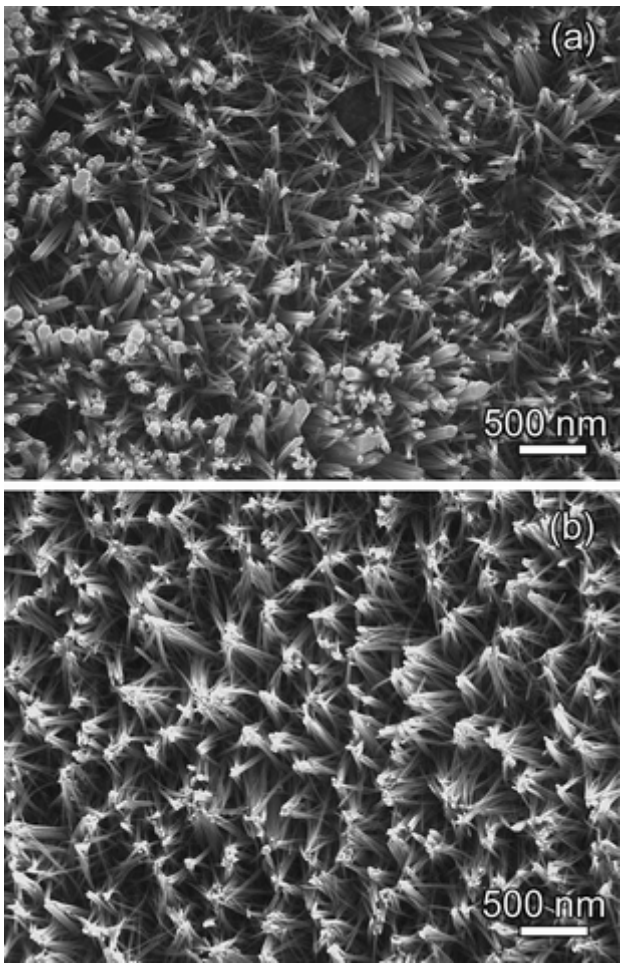

Fig. 10SEM images of nanorod arrays prepared on (a) as purchased Zn foil, and (b) electro polished Zn foil. Other synthesis conditions for the nanorod arrays were kept same, *i.e.* 21 °C, with mixed aqueous solution of 5 mL 0.25% H_2O_2 and 10 mL 0.2M NaOH. The nanorod array on polished Zn foil has better uniformity.

4.5. Different luminescence properties for nanorods with different diameter

The defect luminescence of the ZnO nanorods should be coming from both the surface and the interior of the nanorods. We have attempted surface passivation of the nanorods using SiO_2, when only some improvement on the ZnO band edge emission and suppression of the defect emission is achieved, indicating the nanorod interior also have contribution to the defect emission. The larger-diameter nanorods are grown under higher temperature (150 °C). In addition, the concentration of the oxidant H_2O_2 is relatively higher for the larger-diameter nanorod growth. The more abundant oxidation source and the higher temperature help to reduce the native point defect

formation in the ZnO nanorods, and lead to their improved electronic structure quality. This explains the much stronger band edge emission and weaker defect emission (mainly from intrinsic defects) in the larger-diameter nanorods. In addition, the surface to volume ratio is also significantly increases in the smaller-diameter nanorods, when surface defect luminescence could also make a contribution.[12]

Here, we can see the size of the as prepared ZnO nanorods array have a significant influence on the physical properties of nanomaterials. The controlled fabrication of ZnO nanostructures with desired morphology and sizes is very important for applications such as bio-/gas sensors, hydrogen storage, optoelectronics devices and so on.[18,19]

5. Conclusion

ZnO nanorod arrays on conducting substrates are demonstrated using a solution chemistry approach. The nanorod arrays are uniformly distributed on entire surface of the foil. By systematically varying the synthesis temperature, the relative concentrations of H_2O_2 and NaOH, we found that the average diameter of the ZnO nanorods can be tuned from ~150 nm to ~20 nm. Larger-diameter nanorods are found to possess higher band edge to defect emission ratio, indicating their better electronic structural quality, which is determined by both the growth conditions and the nanorod surface-to-volume ratio. Electrical measurements on single nanorods and its junction with the substrate show ohmic contact between the rods and the substrate, with the resistivity of the nanorods estimated as $\sim 10^{-1}\ \Omega$ cm. Such a growth methodology can be simply applied to many conducting substrates. The ZnO nanorods on conducting substrate with ohmic contact between them provide a feasible configuration for possible nanoelectronic devices.

Acknowledgements

This work is supported by grants from the General Research Fund of Hong Kong SAR under project no. 400207, 414908, and 414709, and CUHK Focused Investment Scheme C.

References

1 Pai-Chun Chang,Zhiyong Fan,Dawei Wang,Wei-Yu Tseng,Wen-An Chiou,Juan Hong and Jia G. Lu, *Chem. Mater.*, 2004, **16**, 5133 [Links].

2 Yanhong Tong,Yichun Liu,Lin Dong,Dongxu Zhao,Jiying Zhang,Youming Lu,Dezhen Shen and Xiwu Fan, *J. Phys. Chem. B*, 2006, **110**, 20263 [Links].

3 C. R. Gorla,N. W. Emanetoglu,S. Liang,W. E. Mayo,Y. Lu,M. Wraback and H. Shen, *J. Appl. Phys.*, 1999, **85**, 2595 [Links].

4 Ü. Özgür,Ya. I. Alivov,C. Liu,A. Teke,M. A. Reshchikov,S. Doğan,V. Avrutin,S.-J. Cho and H. Morkoç, *J. Appl. Phys.*, 2005, **98**, 041301 [Links].

5 Xudong Wang,Jinhui Song,Christopher J. Summers,Jae Hyun Ryou,Peng Li,Russell D. Dupuis and Zhong L. Wang, *J. Phys. Chem. B*, 2006, **110**, 7720 [Links].

6 Jinping Liu,Xintang Huang,Yuanyuan Li,Xiaoxu Ji,Zikun Li,Xiang He and Fenglou Sun, *J. Phys. Chem. C*, 2007, **111**, 4990 [Links].

7 Xiaogang Wen,Yueping Fang,Qi Pang,Chunlei Yang,Jiannong Wang,Weikun Ge,Kam Sing Wong and Shihe Yang, *J. Phys. Chem. B*, 2005, **109**, 15303 [Links].

8 Jinhu Yang,Guangming Liu,Jun Lu,Yongfu Qiu and Shihe Yang, *Appl. Phys. Lett.*, 2007, **90**,

103109 [Links].
9 Youngjo Tak and Kijung Yong, *J. Phys. Chem. B*, 2005, **109**, 19263 [Links].
1 Xudong Wang,Jinhui Song,Peng Li,Jae Hyun Ryou,Russell D. Dupuis,Christopher J.
0 Summers and Zhong L. Wang, *J. Am. Chem. Soc.*, 2005, **127**, 7920 [Links].
1 L. Shi,Y. M. Xu and Q. Li, *Appl. Phys. Lett.*, 2007, **90**, 211910 [Links].
1
1 K. H. Tam,C. K. Cheung,Y. H. Leung,A. B. Djurisic,C. C. Ling,C. D. Beling,S. Fung,W. M.
2 Kwok,W. K. Chan,D. L. Philips,L. Ding and W. K. Ge, *J. Phys. Chem. B*, 2006, **110**, 20865 [Links].
1 D. Li,Y. H. Leung,A. B. Djuri š iæ,Z. T. Liu,M. H. Xie,S. L. Shi,S. J. Xu and W. K. Chan,
3 *Appl. Phys. Lett.*, 2004, **85**, 1601 [Links].
1 L. Shi,Y. M. Xu,S. K. Hark,Y. Liu,S. Wang,L. M. Peng,K. W. Wong and Q. Li, *Nano Lett.*,
4 2007, **7**(12), 3559 [Links].
1 Feng Xu,Yinong Lu,Yan Xie and Yunfei Liu, *J. Phys. Chem. C*, 2009, **113**, 1052 [Links].
5
1 W. Ostwald, *Lehrbuch der Allgemeinen Chemie* 1896, vol. 2, part 1. Leipzig, Germany.
6
1 J. C. Brice, *Crystal Growth Processes*, Halsted Press, 1986, pp 194–211.
7
1 J. H. Zhang,H. Y. Liu,Z. L. Wang,N. B. Ming,Z. R. Li and A. S. Biris, *Adv. Funct. Mater.*,
8 2007, **17**, 3897 [Links].
1 J. H. Zhang,H. Y. Liu,Z. L. Wang and N. B. Ming, *Appl. Phys. Lett.*, 2007, **90**, 113117
9 [Links].